This article has been accepted for publication in IEEE Journal of Electromagnetics, RF and Microwaves in Medicine and Biology. This is the author's version which has not been fully edited content may change prior to final publication. Citation information: DOI 10.1109/JERM.2024.3363906

High-speed thermal imaging can resolve short RF pulse effects in tissue models

Daniel W. van der Weide, *Fellow, IEEE,* Dustin Kendig, and Mo Shakouri, *Member, IEEE*

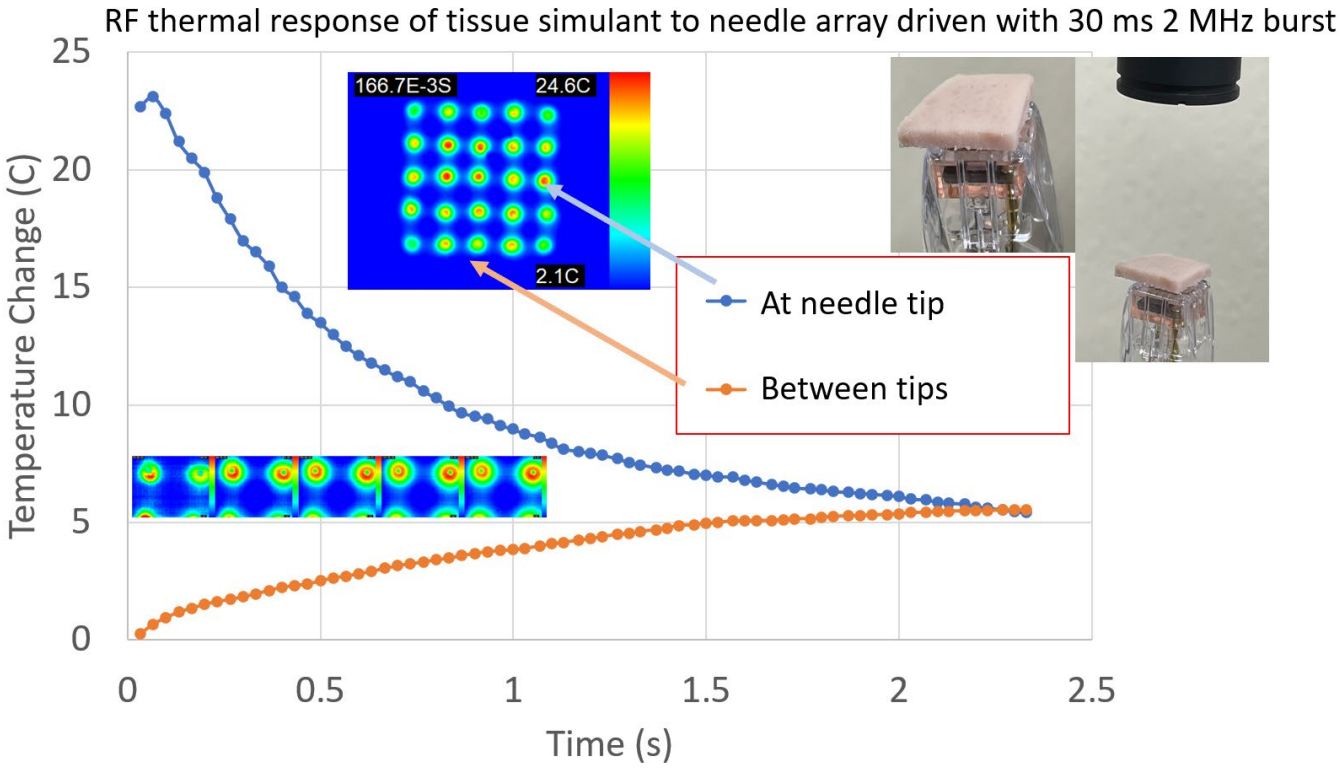

Take-Home Messages

- Using fast and high-resolution thermal imaging lets us track RF-induced heating separately from conductive diffusion
- RF-excited bipolar needles show rapid and localized temperature rise around them with only slow diffusion of heat between them
- Sliced processed ham has RF conductivity and permittivity comparable to porcine skin and serves as a useful tissue simulant for thermal mapping with advanced transient (thermoreflectance/infrared) microscope
- We find that IR was sufficient for the time and length scales of this experiment, while thermoreflectance in the same instrument will enable higher spatial and temporal resolution for future experiments

High-speed thermal imaging can resolve short RF pulse effects in tissue models

Daniel W. van der Weide, *Fellow, IEEE,* Dustin Kendig, and Mo Shakouri, *Member, IEEE*

***Abstract*— Using high-speed transient infrared microscopy, we resolve induced heating and subsequent conductive diffusion of pulsed RF energy delivered by bipolar microneedles to tissue-mimicking samples, using high spatial and temporal resolution, non-contact advanced thermal imaging to gain insight into direct heating of tissue proximal to RF electrodes. We use both IR and thermoreflectance in the same microscope and find that for the samples and time scales chosen in this first study, the spatiotemporal resolution of IR microscopy was sufficient to reveal local RF-induced thermal effects.**

***Keywords* — transient IR, thermoreflectance, infrared, RF heating, RF tissue effects, microneedles**

I. Introduction

Understanding the effects of high-frequency (RF or microwave) energy on tissue for both diagnostics and therapeutics [1] has become increasingly important as new techniques both emerge and may even become health concerns [2]. One such cosmetic application of RF energy is for rejuvenation of skin, in which it is applied via microneedle electrodes through the epidermis to the dermis to locally increase tissue temperature, inducing thermal injury to dermal collagen and provoking a healing response that in turn can cause a reduction in the appearance of wrinkles [3]. Like most therapeutic applications of RF or microwave energy, this involves direct (induced) and diffusive (conductive) thermal effects, which may both (or either) be desired and/or mask underlying non-thermal tissue transformation.

Both thermal and less-familiar non-thermal effects of RF and microwave exposure have been comprehensively reviewed in a recent article by Hirata *et al.* [4]. While theoretical investigations have been published [5], experimentally disentangling the direct (induced) *vs.* conductive (diffusive) thermal from non-thermal tissue response has been limited in reports [6] that employ conventional thermal sensing and imaging techniques found in many IR cameras *vs.* the transient microscopy techniques described here..

Alternatively, in pursuit of higher resolution, accuracy and speed, instrumenting actual tissue or phantoms with point sensors such as thermocouples also interferes with and tends to localize electric fields, while fiber optic temperature sensors are stiff and brittle; neither of these point sensors is non-invasive.

For example, the recent (2023) study of fractional[2] RF treatment with microneedles [6] used *ex vivo* bovine liver tissue and thermometrically evaluated temperature changes elicited in the tissue with a conventional thermal imaging camera (FLIR E5; FLIR Systems Inc., Wilsonville, OR, USA). Although the 10,800-pixel (120×90) camera used had a sensitivity of less than 0.10°C, its spatial and temporal resolution were insufficient to appreciate the contrast between direct and diffusive RF heating at <0.3-mm needle-diameter resolution; rather, the images provided in this reference show only the broad temperature changes at the 10×10 mm size of the needle array; it did not reveal the fractional nature of treatment. This limited spatial resolution was accompanied by images taken at 10 s intervals, also insufficient to distinguish the effects of diffusion from the immediate and direct RF heating of tissue by the energized needles themselves.

Beyond achieving a more accurate understanding of heat distribution in tissue, however, mapping the short-time temperature distribution of RF energy is important for dosing [7]. This is particularly important for precise and localized tissue injury (*e.g.,* for skin rejuvenation) [8].

In this work, we apply transient infrared (IR) microscopy with temperature resolution comparable to conventional IR cameras but with 5 μm spatial and 50 μs temporal resolution. Depending on the speed of the sample's thermal response, we can apply the same instrument to both quantitatively image using IR emission and thermoreflectance to reveal the localized effect of direct RF tissue heating at the needle electrodes *vs.* the subsequent diffusion after the RF excitation is removed.

This paper is an extension of a post-deadline presentation at the IMBioC 2023, Leuven, Belgium. Daniel W. van der Weide is with University of Wisconsin-Madison, WI 53706 USA (e-mail: danvdw@engr.wisc.edu).

Dustin Kendig and Mo Shakouri are with MicroSanj LLC, Fremont, CA 94538 USA

[2] "Fractional" treatment addresses finite points in a treatment area, addressing a (small) fraction of the total area to recruit a healing response.

II. Experimental Setup

A. Background of transient IR

Transient IR microscopy uses both IR emission and thermoreflectance, depending on the speed of the sample's response. While IR imaging is more familiar and was the primary modality for the results shown here, thermoreflectance imaging is a newer optical technique used to measure thermal properties and temperature profiles on the surface of materials and devices at shorter timescales, and it can be seamlessly applied and compared with IR emission as the sample volume shrinks and speed of thermal response increases. As indicated in Figure 1, it is based on the principle that the reflectivity of a material changes slightly with temperature.

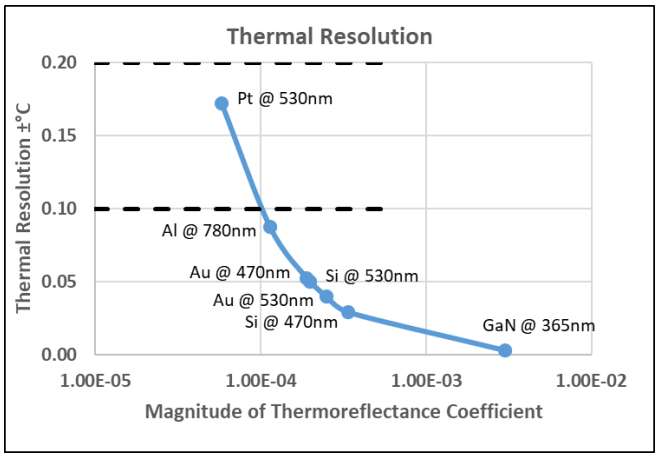

Fig. 1. Dependence of thermal resolution on thermoreflectance coefficient for certain metals and semiconductor materials at given illumination wavelengths [9, 10].

The basic process involves shining a modulated light source onto the sample surface and measuring the reflected intensity using a photodetector or imaging array. As the sample temperature changes, small changes in reflected light intensity are measured. These thermoreflectance signals are then analyzed to extract quantitative information about thermal conductivity, heat capacity, and temperature profiles of the sample.

Advantages of transient IR microscopy over point sensors are especially relevant in this evaluation of skin-treatment devices: such imaging is a non-contact and non-destructive measurement technique. This allows testing without physically contacting or altering them. Moreover, it has high spatial resolution on the micron scale, enabling high resolution thermal imaging and mapping of heat distribution.

In summary, transient IR microscopy using thermoreflectance/IR offers a fast, calibrated, non-contact imaging technique that has until now been applied primarily to semiconductor and other electronic devices and circuits to overcome limitations of conventional infrared thermography [9, 10].

B. Instrument configuration

As shown in Figure 2, to configure transient IR microscopy for mapping the induced heat distribution in simulated tissue due to RF-excited bipolar microneedle electrodes, we used a commercially available TR/IR microscope (MicroSanj EZ-500). While thermoreflectance images can be calibrated with reference to the IR emission and were initially evaluated here, we found that the temporal response of the sample chosen was slow enough for IR (due to its mass and homogeneity relative to typical inorganic circuit samples), and IR consequently gave images with larger signal to noise ratio (SNR). We expect that as the sample homogeneity and thermal mass decreases (speeding up sample's thermal response), the thermoreflectance images will provide greater temporal and spatial resolution, albeit at reduced signal levels.

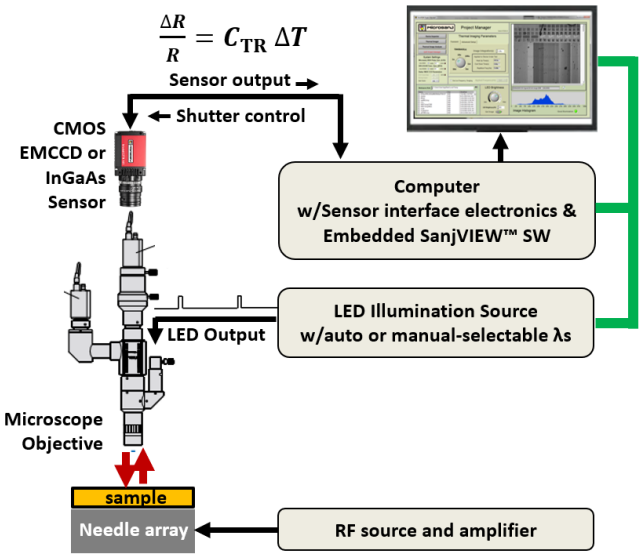

Fig. 2. Transient IR (thermoreflectance/infrared) measurement system and experimental setup (EZ-500); R = reflectance; T = temperature; C_{TR} = thermoreflectance coefficient.

Applicators for skin rejuvenation procedures are typically arrays of 0.3 mm diameter microneedles that provide fractional RF treatment of the dermis in pulses or tone bursts lasting several tens to hundreds of ms. As shown in Figure 3, a sample of tissue simulant is mounted onto an applicator microneedle array (Serendia Sylfirm X25) so that the tips of the needles are nearly flush with the top surface of the sample. We connected a flexible coaxial cable to the two (+ and -) driving electrode pins of the array (normally driven by a handpiece itself connected to a custom RF generator) that themselves each drive half of the needle electrodes, which are wired with interleaved, alternating polarities in a checkerboard pattern such that the polarities of the array of needles is bipolar, and there is no need for a ground return.

The RF source was a Keysight N5171B signal generator exciting an AR/Kalmus LA500H RF power amplifier (gain 57 dB) differentially driving the input electrodes of the microneedle array to apply RF pulses to a ~5 mm thick

tissue simulant; the needles were extended by their full 4 mm length and their tips made flush with the slightly compressed sample surface. We then imaged the result over a 2.4 s interval using a MicroSanj EZ500 thermal imaging system and SanjVIEW thermal analysis tool. In another test we used a 120 ms burst of RF to create higher temperatures; results of that are shown below in portions of Figure 6 and Figure 7.

C. *Tissue simulant*

Access to tissue models that can represent skin-like RF dielectric and conductivity for experiments like these is limited. To promote repeatability, we chose readily available supermarket Oscar Meyer Lean Ham slices, which proved to be of uniform consistency and thickness (~2.5 mm per slice).

It is useful to consider how closely this simulant's dielectric properties agree with literature. While the circa-2006 permittivity and conductivity data of *in-vivo* forearm skin from Gabriel *et al.* [11] (measured with a coaxial probe) is often cited as a benchmark, the tissue model we choose is much closer to Sasaki's 2014 data of *in-vitro* porcine epidermis (quoted in [12]). Using a parallel-plate fixture, we measured our tissue model from 75 kHz to 7 MHz using an HP 4285A Precision LCR Meter to characterize the low-frequency dielectric permittivity and conductivity of a two-slice stack as was used in the experiments (Figure 3). At 2 MHz, the Gabriel skin data indicates relative permittivity $\varepsilon_r \sim 500$, while extrapolation of Sasaki's data is comparable to our parallel-plate value of $\varepsilon_r \sim 300$. Likewise, the Gabriel conductivity value at 2 MHz is $\sigma \sim 0.3$ S/m, while extrapolation of Sasaki's data is comparable to our parallel-plate value of $\sigma \sim 0.1$ S/m.

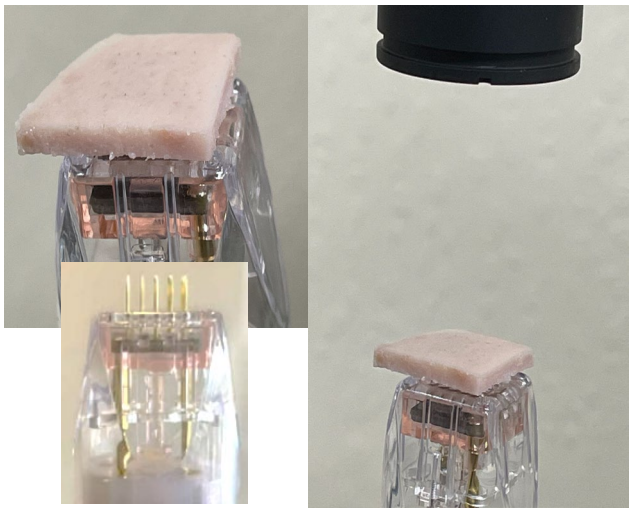

Fig. 3. Detail of tissue simulant mounted onto microneedle array (left). Imaging lens positioned above sample (right). Power is delivered via coaxial cable (not shown) connected to the two lower pins visible through the plastic housing of the needle array (lower left photo).

III. Thermal Results

To evaluate both how heat is generated through RF microneedles and how it subsequently diffuses in the sample, we applied to the needle array a typical treatment schedule of a 30 ms tone burst of 2 MHz with a peak voltage $V_p \approx 70$ V (48 W average power into 50 Ω with negligible measurable reflected power), and noted a rapid rise in temperature around the needle tips to a peak temperature of 28.3 °C above ambient, decaying with a time constant of ~0.77 s. Meanwhile, the temperature measured between the needles rose from ambient (~21 °C) by 5 °C over the course of a 2.4 s window, as shown in Figure 4. We also applied another typical treatment of a 120 ms burst of the same power and frequency of RF to create higher temperatures in a higher spatial resolution experiment; results of that are shown Figure 6 and in the lower row of Figure 7.

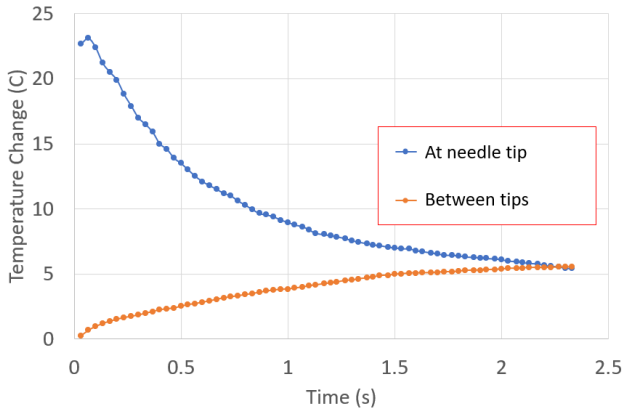

Fig. 4. Peak temperature adjacent to a needle tip and temperature between needles in tissue simulant after 30 ms, 48 W, 2 MHz pulse.

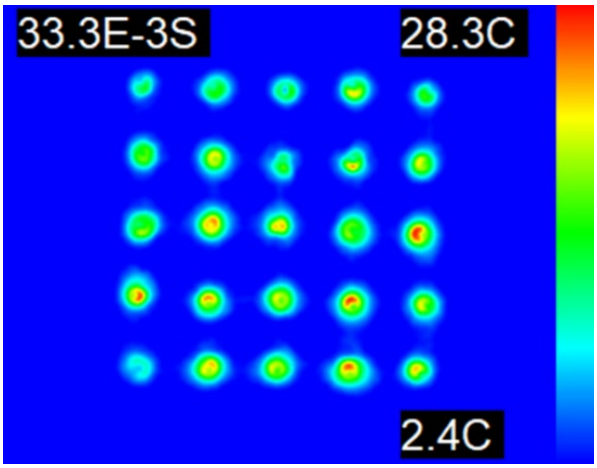

Fig. 5. Image of temperature distribution in sample after 30 ms pulse showing lowest (2.4 C above ambient) and highest (28.3 C above ambient) temperatures.

Figure 5 displays the image of the peak temperature distribution in the sample, which occurs at 33 ms. Figure 6 shows 33 ms intervals both overall and at higher magnification, showing the detailed distribution of temperature between two adjacent needle tips, whose pitch is 2 mm (recall that the higher-magnification images were taken with a 120 ms pulse, thus reaching higher temperatures). Figure 7 shows the detail of the needle tips for the right-most frame of Figure 6. It is notable that the

needle tips themselves are cooler than their immediate surroundings, indicating that the RF energy is exciting the peak temperature adjacent to a needle tip via induction, while conductive diffusion raises the temperature between needles slowly toward equilibrium (Figure 4). This level of spatiotemporal detail of RF application to microneedles in tissue has not previously been reported. While we found that transient IR microscopy gave better SNR at these time and length scales for this homogeneous sample, we expect that at much higher spatial and temporal resolution, establishing a baseline with IR and then using faster thermoreflectance imaging will provide even greater detail.

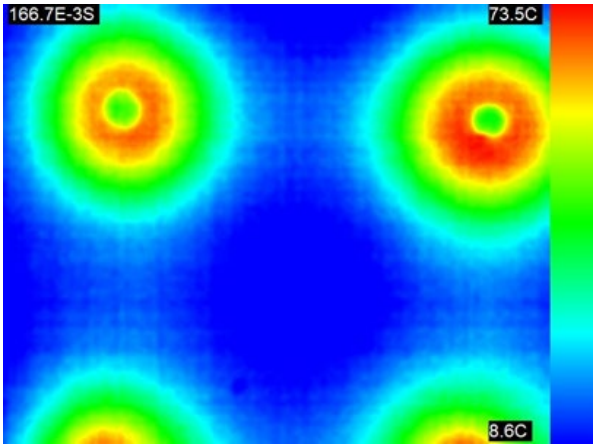

Fig. 6. High-magnification detail at 5 mm/pixel for the 167 ms frame. Green circles at the center of the images are the needle tips. Needles are at 2 mm pitch. Temperatures shown are above ambient.

IV. CONCLUSIONS

We have shown high temporal, spatial and thermal resolution images for RF excitation of a tissue simulant, the first application of a semiconductor/device thermal microscope to an RF tissue treatment modality. The results reveal distinctions between RF-induced heating and subsequent conductive thermal diffusion at new resolutions and timescales that will help illuminate the effects of RF in tissue. While here we found that IR microscopy offers sufficient temporal and spatial resolution with a minimum of noise, thermoreflectance will address the few-micron length scales and hundred-nanosecond timescales of future studies.

ACKNOWLEDGMENT

The authors would like to thank Yuchen Gu at University of Wisconsin-Madison for his help with tissue characterization.

REFERENCES

[1] C. L. Brace, P. F. Laeseke, D. W. van der Weide, and F. T. Lee, "Microwave ablation with a triaxial antenna: results in ex vivo bovine liver," IEEE Transactions on Microwave Theory and Techniques, vol. 53, no. 1, pp. 215-220, 2005.

[2] J. C. Lin, "Microwave Auditory Effects Among U.S. Government Personnel Reporting Directional Audible and Sensory Phenomena in Havana," IEEE Access, vol. 10, pp. 44577-44582, 2022.

[3] P. G. Vassão et al., "Radiofrequency and skin rejuvenation: a systematic review," Journal of Cosmetic and Laser Therapy, vol. 24, no. 1-5, pp. 9-21, 2022.

[4] A. Hirata et al., "Assessment of Human Exposure to Electromagnetic Fields: Review and Future Directions," IEEE Transactions on Electromagnetic Compatibility, vol. 63, no. 5, pp. 1619-1630, 2021.

[5] W. Schramm, D. Yang, and D. Haemmerich, "Contribution of Direct Heating, Thermal Conduction and Perfusion during Radiofrequency and Microwave Ablation," in 2006 International Conference of the IEEE Engineering in Medicine and Biology Society, 30 Aug.-3 Sept. 2006 2006, pp. 5013-5016.

[6] M. Choi, H. S. Lee, and S. B. Cho, "Effect of Pulse Widths and Cycles on Invasive, Bipolar, and Gated Radiofrequency-Induced Thermal Reactions in ex vivo Bovine Liver Tissue," Clinical, Cosmetic and Investigational Dermatology, vol. Volume 16, pp. 87-97, 2023-01-01 2023, doi: 10.2147/ccid.s395072.

[7] D. Berube, B. Renton, and B. M. Hantash, "A predictive model of minimally invasive bipolar fractional radiofrequency skin treatment," Lasers in Surgery and Medicine, vol. 41, no. 7, p. 473, 2009.

[8] J. Na, Z. Zheng, C. Dannaker, S. E. Lee, J.-S. Kang, and S. B. Cho, "Electromagnetic Initiation and Propagation of Bipolar

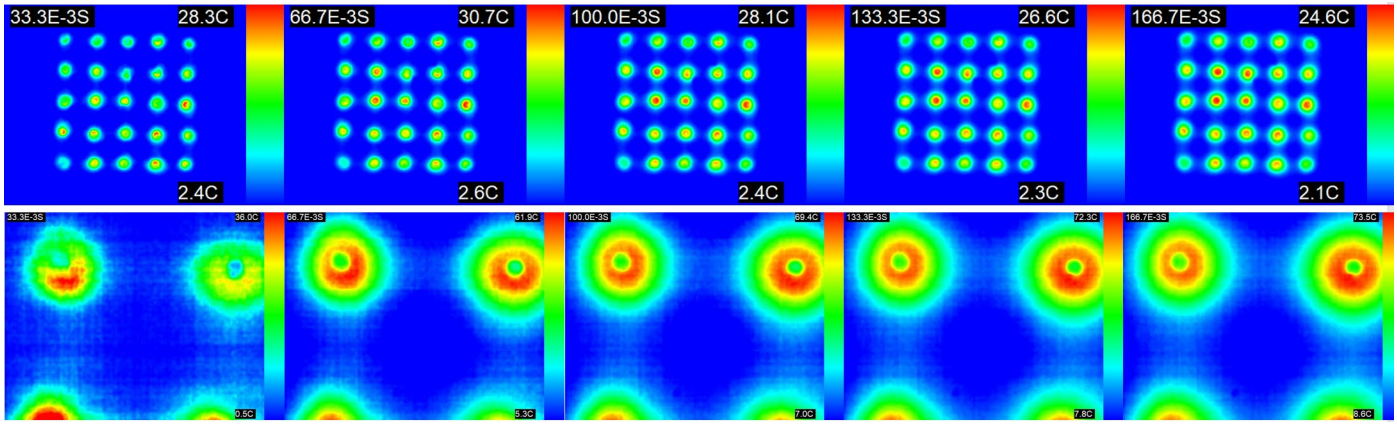

Fig. 7. Evolution of temperature distribution for a 30 ms pulse at 33 ms intervals (top row) and high-magnification detail for a 120 ms pulse at 5 mm/pixel (bottom row). The temperatures shown are above ambient.

Radiofrequency Tissue Reactions via Invasive Non-Insulated Microneedle Electrodes," Scientific Reports, vol. 5, no. 1, p. 16735, 2015/11/13 2015, doi: 10.1038/srep16735.

[9] D. Kendig, G. Hohensee, E. Pek, W. Kuang, K. Yazawa, and A. Shakouri, "Accurate thermoreflectance imaging of nano-features using thermal decay," in 2017 16th IEEE Intersociety Conference on Thermal and Thermomechanical Phenomena in Electronic Systems (ITherm), 30 May-2 June 2017, pp. 23-29.

[10] D. Kendig, K. Yazawa, and A. Shakouri, "Hyperspectral thermoreflectance imaging for power devices," in 2017 33rd Thermal Measurement, Modeling & Management Symposium (SEMI-THERM), 13-17 March 2017 2017, pp. 204-207.

[11] S. Gabriel, R. W. Lau, and C. Gabriel, "The dielectric properties of biological tissues: II. Measurements in the frequency range 10 Hz to 20 GHz," vol. 41, no. 11, pp. 2251-2269, 1996.

[12] K. Sasaki, E. Porter, E. A. Rashed, L. Farrugia, and G. Schmid, "Measurement and image-based estimation of dielectric properties of biological tissues —past, present, and future—," Physics in Medicine & Biology, vol. 67, no. 14, p. 14TR01, 2022.

Daniel W. van der Weide (M'87–SM'16–F'22) received the B.S.E.E. degree from The University of Iowa, Iowa City, IA, USA, in 1987, and the master's and Ph.D. degrees in electrical engineering from Stanford University, Stanford, CA, USA, in 1989 and 1993, respectively. He held positions at the Lawrence Livermore National Laboratory, Livermore, CA, USA, Hewlett-Packard, Santa Rosa, CA, USA, Motorola, Schaumburg, IL, USA, and Watkins-Johnson Company, Palo Alto, CA, USA. From 1993 to 1995, he was a Post-Doctoral Researcher with the Max-Planck-Institute for Solid State Research, Stuttgart, Germany.

He then joined the Department of Electrical and Computer Engineering, University of Delaware, Newark, DE, USA, as an Assistant Professor, where he was promoted to Associate Professor while founding and directing the Center for Nanomachined Surfaces. In 1999, he moved to the University of Wisconsin–Madison, Madison, WI, USA, where he is currently a Full Professor of electrical and computer engineering. He is also a Co-Founder of Neuwave Medical Inc., Madison (acquired by Johnson & Johnson in 2016), Optametra LLC, Verona, WI, USA (acquired by Tektronix in July 2011), Tera-X LLC, Verona, and, most recently, Elucent Medical, Eden Prairie, USA, Accure, Madison, USA and ANTENNEX, Eindhoven, NL.

Dr. van der Weide received the PECASE Award from the National Science Foundation in 1997, the DARPA Ultra Electronics Program Outstanding Individual Technical Achievement Award in 1997, and the Young Investigator Program Award from the Office of Naval Research in 1998.

Dustin Kendig received his B.S. degree with Honors in Electrical Engineering from the University of California, Santa Cruz in 2009. He is Co-Founder and Vice President of Microsanj LLC in Santa Clara, California. At Microsanj he is developing sub-micrometer transient thermal imaging systems for the semiconductor industry for thermal characterization and fault isolation. Microsanj has 75+ commercial products and research partnerships with companies and research labs in a dozen countries. He is a member of the IEEE Instrumentation and Measurement and Reliability Societies. In 2009, he was the recipient of the Huffman Prize, Dean's Award, and Chancellor's Award. He won best poster at IEEE PVSC in 2010 and best paper at IEEE ITherm in 2017. He holds 4 patents and has published over 60 papers.

Mo Shakouri is co-founder, President & CEO of Microsanj LLC, a leading supplier of high resolution, thermal imaging systems designed to address the thermal challenges faced by today's advanced device designers. Dr. Shakouri received his PhD from Stanford University and has more than 20 years of experience directing major programs with Hewlett-Packard Corporation, Lucent Technologies, and Alvarion Corporation prior to the founding of Microsanj in 2007. Mo also serves as CEO for Telewave.io, which designs and manufactures high quality products for RF networks. Mo is also the Board Chairman for the WiMAX Forum, an industry trade organization formed by leading communications, component, and equipment companies to promote and certify compatibility and interoperability of broadband wireless access equipment that conforms to the IEEE 802.16 and ETSI HiperMAN standards.